# Efficient Catalytic Plasma Activation of $CO_2$, NO, and $H_2O$

**Steven L. Suib,*,†,‡ Stephanie L. Brock,† Manuel Marquez,†,§ Jian Luo,† Hiroshige Matsumoto,†,|| and Yuji Hayashi▽**

*Department of Chemistry, U-60, University of Connecticut, Storrs, Connecticut 06269-4060, Department of Chemical Engineering and Institute of Materials Science, University of Connecticut, Storrs, Connecticut 06269-4060, Department of Electrical Engineering and Applied Physics, Yale University, New Haven, Connecticut 06511, Department of Chemistry, Nagasaki University, Bunkyomachi 1-14 Nagasaki 852, Japan, and Fujitsu Laboratories, Ltd., 1015 Kamikodanaka, Nakahara 211, Japan*

*Received: May 12, 1998; In Final Form: July 30, 1998*

The activation of small molecules, such as $CO_2$, NO, and $H_2O$, has been achieved at atmospheric pressure via ac glow discharge methods in the presence of metal catalysts coated onto the electrode surfaces. A fan-type reactor having one rotating and one static electrode has been designed to diminish mass transfer effects. Time lapse photography of the emitting plasma intermediate species and optical emission studies have been used to monitor reaction pathways. Gas chromatography, mass spectrometry, and combined GC−MS methods have been used to monitor product distributions, selectivities, and activities. The effects of flow rate, input voltage, diluent gases, and metal coating have been systematically studied. Additionally, the mechanisms of $CO_2$ decomposition and the role of the metal catalyst in that decomposition have been studied by optical emission spectroscopy.

## Introduction

Activation of small stable abundant molecules such as $CO_2$, $H_2O$, and $CH_4$ has been the focus of considerable attention of researchers in the areas of synthesis, catalysis, energy conversions, environmental monitoring, as well as other areas.[1−5] The selective activation of one bond, or a selective generation of a particular product or set of products, has been a major focus of such research.

Selective synthesis and the mechanism of formation of high value products from such small molecules is the focus of our research. While thermal, electrochemical, and photochemical methods have led to significant advances in selective activation of several stable organic and inorganic small molecules, inherent limitations such as low activity, high cost, and limited possibilities for the scale-up of such methods exist. For example, it is difficult to selectively activate $CO_2$ or $CH_4$ with thermal methods,[6] and electrochemical methods are not commercially practical due to the high cost of electricity, with the noted exception of the KetChlor process for formation of $Cl_2$ from HCl.[7] Finally, the scale-up of photochemical reactions is difficult due to loss of light via scattering and absorption and heat loss. One exception is the photonitrosation of cyclohexane for the production of cyclohexanone oxime via the Toray PNC process.[8]

Cold plasmas can be used to activate gaseous species and, in certain cases, nonthermodynamic equilibria can be obtained to selectively activate stable small molecules.[9] Various types of energy and radiation can be used such as microwaves,[10,11] radio frequency,[12] and electricity[13,14] to generate such plasmas. A limited number of studies in microwave and radio frequency catalysis are available due to problems associated with low yields from use of low pressure, mass transfer limitations, deactivation via formation of coke, or deposition on electrodes, and high operational costs.

Rotating and stator electrodes in ac glow discharges can be used to minimize and solve many of these problems. Metals can be coated onto electrode surfaces that may act as catalysts. Reactions can be done at atmospheric pressure, good mixing can be obtained by using high rotation rates, and degradation of the electrodes, which occurs in dc sputtering, can be minimized. The costs of such instrumentation are also considerably lower than for microwave or radio frequency equipment.

Here we describe the decomposition of $CO_2$, NO, and $H_2O$ in fan-type[15] ac glow discharge plasmas at atmospheric pressure. The influence of flow rate, input voltage, diluent gas, and metal coating of the electrode on conversions are discussed along with optical emission studies, which provide insight into the mechanism of $CO_2$ decomposition and the role the metal catalyst plays in the activation of $CO_2$.

## Experimental Section

**General.** The fan-type reactor consists of an inner rotor with 10 fan blades separated by a gap of 0.3 mm from the outer stator. Both rotor and stator have been coated with a variety of metal coatings (Au, Pt, Pd, Rh, Cu, Ni, Fe) using electroless plating. The rotation is controlled by a motor placed inside the rotor, and the fan speed is maintained at 3600 rpm. The outer diameter of the rotor is 6.27 cm (including the fan blades), the inner diameter of the stator is 6.33 cm, and the length of the reactor is 1.66 cm, producing a plasma volume of approximately 0.26 $cm^3$. Experiments were conducted with a Japan-Inter uHV-10 8.1 kHz ac high voltage generator and the voltage conditions were monitored using a Tektronix 6015A high voltage probe and a Yokogawa digital oscilloscope DL

* To whom correspondence should be addressed.
† Department of Chemistry, University of Connecticut.
‡ Department of Chemical Engineering and Institute of Materials Science.
§ Department of Electrical Engineering and Applied Physics.
|| Department of Chemistry, Nagasaki University.
▽ Fujitsu Laboratories, Ltd.

10.1021/jp9822079 CCC: $15.00 
Published on Web 11/04/1998

**TABLE 1: Conversion of $CO_2$ and Rates of $CO_2$ Consumption for Fan-Type Reactors as a Function of Metal Coating, Root-Mean-Square Input Voltage (rms, $V_{in}$) and Flow Rate for a 2.5% $CO_2$ in He Mixture**

| | | flow rate | | | | | |
|---|---|---|---|---|---|---|---|
| | | 30 cc/min | | 60 cc/min | | 100 cc/min | |
| metal | rms $V_{in}$ (V) | conversion (%) | $CO_2$ consumed (g/1000 h) | conversion (%) | $CO_2$ consumed (g/1000 h) | conversion (%) | $CO_2$ consumed (g/1000 h) |
| Au | 411 | 7.2 | 5.8 | 4.5 | 7.3 | 2.8 | 7.7 |
| | 711 | 11.5 | 9.4 | 8.1 | 13.3 | 5.0 | 13.6 |
| | 906 | 15.2 | 12.4 | 9.4 | 15.3 | 5.0 | 13.6 |
| Pd | 411 | 8.1 | 6.6 | 6.1 | 10.5 | 4.1 | 11.2 |
| | 711 | 15.8 | 12.8 | 10.1 | 17.3 | 7.2 | 19.7 |
| | 906 | 20.9 | 17.0 | 13.6 | 23.3 | 9.9 | 26.9 |
| Pt | 411 | 11.7 | 9.5 | 7.8 | 12.7 | 3.8 | 10.4 |
| | 711 | 20.5 | 16.6 | 14.1 | 22.9 | 7.8 | 21.2 |
| | 906 | 24.1 | 19.6 | 16.7 | 27.2 | 11.1 | 30.2 |
| Rh | 411 | 10.6 | 8.6 | 6.9 | 11.2 | 5.8 | 16.5 |
| | 711 | 21.6 | 17.6 | 13.2 | 21.5 | 10.5 | 30.5 |
| | 906 | 30.5 | 24.9 | 16.6 | 27.1 | 12.4 | 35.5 |

1520. The current across the reactor was measured from the voltage drop across a standard 10 Ω resistor. The power consumed by the plasma was obtained by integrating the product of voltage and current as a function of time.

**$CO_2$ Dissociation Studies**. The root-mean-square (rms) input voltages were varied between 411 and 906 V, using flow rates ($Q$) between 30 and 100 $cm^3$/min. Gas mixtures containing $CO_2$ concentrations of between 0.5 and 4% of $CO_2$ in He, Ar, or $N_2$ were used as the feed and all reactions were conducted at atmospheric pressure. The feed and product gases were monitored using an MKS−UTI PPT quadrupole residual gas analyzer mass spectrometer with a Faraday cup detector and a variable high-pressure sampling manifold.

Optical emission spectroscopy studies were carried out in the 200−900 nm range using a 270 M Spex instrument with a CCD detector. Note that the optical phenomena described here are unique from emission spectroscopy spark−arc experiments and might more appropriately be termed luminescence. Light emitted from the plasma is collected and directed to the monochromator with a fiber optic cable. The He emission lines in the spectra are accurate to ±0.1 nm.

**$NO_x$ Remediation and Water Splitting Studies.** The flow rate was varied between 20 and 80 $cm^3$/min for NO (1.0% in He), and 10 and 80 $cm^3$/min for $H_2O$ (2.9−3.1% in He). The input voltage in both cases was 1.29 kV rms. Product analysis was done on-line with an HP-5990A gas chromatograph equipped with a thermal conductivity detector, an HP 3395 integrator, and a 25 ft long packed Carboxcen column.

## Results and Discussion

**$CO_2$ Dissociation.** Emission control of $CO_2$ has become a global concern.[16] The enhanced greenhouse effect due to increased $CO_2$ emission from man-made sources is expected to have profound effects on the global climate.[17] Furthermore, the natural mechanism of $CO_2$ reduction by oceanic uptake is projected to decrease under global warming conditions.[18] Annual decreases in emission over the next century of 50% are required to stabilize the global temperature in its natural range.[16] Recent research directions have focused on trapping and large scale uses of $CO_2$[19] and efficient methods for $CO_2$ decomposition or disposal to try and meet this anticipated demand.[20] One method of $CO_2$ remediation of interest is the conversion of $CO_2$ to CO for energy sources such as synthesis gas and as a reactant to form high energy products. While this route is not economically feasible by thermal methods currently available, activation of $CO_2$ by plasmas should, in principle, provide an inexpensive, clean route to CO.

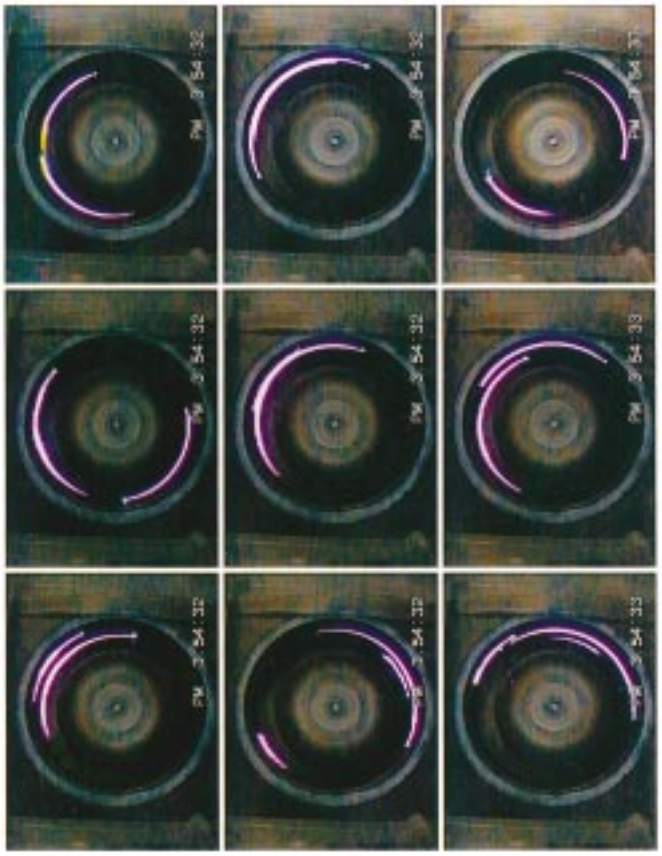

**Figure 1.** Time lapse photo of an ac glow discharge in air taken with a streak camera. Each photo represents an interval of 1/18 s, reading first from left to right then top to bottom.

Time lapse photos of the ac discharge in air of a fan-type plasma reactor in Figure 1 show that the discharge moves around the circumference of the 0.3 mm gap between the outer stator and inner rotor electrode. Such emitting species represent catalytic excited-state atoms, ions, and molecules that are intermediates formed during plasma activation. Conversion and $CO_2$ consumption rates for the ac glow discharge plasma as a function of flow rate and input voltage for selected metal coatings (Au, Pd, Pt, Rh) are presented in Table 1. The data were obtained using a 2.5% $CO_2$ in He feed and the $CO_2$ concentration, as well as those of the products (CO and $O_2$) were monitored by mass spectrometry with a partial pressure analyzer. Comparative studies show that the type of metal coating is significant and that, under optimal conditions, an order

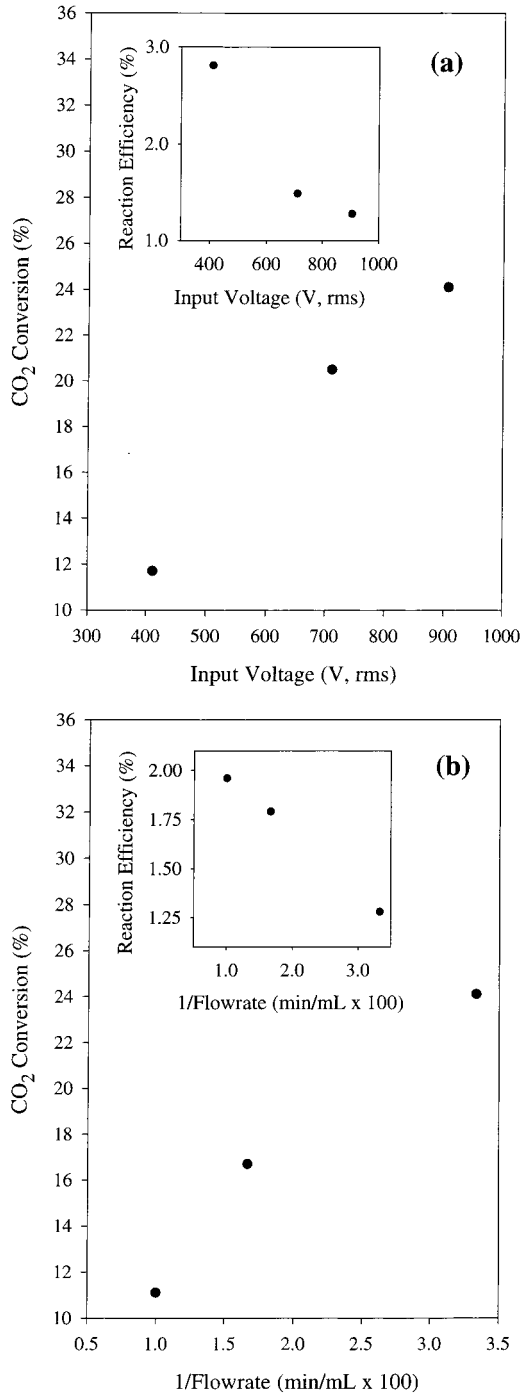


**Figure 2.** Conversion and percent efficiency (inset) data for the decomposition of $CO_2$ using a Pt coated reactor: (a) as a function of input voltage and (b) as a function of inverse flow rate. Efficiencies were calculated from $\Delta H$ for the reaction: $CO_2 \rightarrow CO + O$ (257 kJ/mol), divided by the plasma energy (kJ) per mol of $CO_2$ consumed.

of reactivity of Rh > Pt > Pd > Au exists. Conversions of up to 30.5%, and $CO_2$ consumption rates of up to 35.5 g/1000 h are obtained. Reactions were run continuously for up to 12 h with no change in activity. Figure 2 illustrates the trends in conversion for the Pt reactor, typical for all the reactors studied, as a function of (a) input voltage and (b) inverse flowrate. The highest conversions occur when the flow rate is minimized and the input voltage is maximized. The efficiency of the reaction has been computed as the energy required for the dissociation of $CO_2$ to CO and $O_2$ (257 kJ/mol) divided by the energy of the plasma per mole of $CO_2$ consumed. The percent efficiency

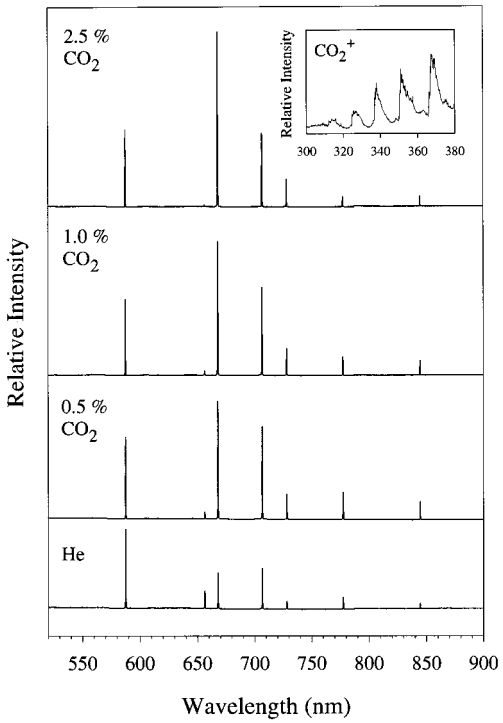


**Figure 3.** Optical emission spectra for pure He, and $CO_2$ in He mixtures (0.5−2.5%) obtained with a gold coated reactor, $V_{in} = 1.07$ kV rms, $q = 30$ cm$^3$/min. Note the large change in relative intensity of the He emission lines as a function of $CO_2$ concentration. The inset shows the excited-state $CO_2^+$ bands, $A^2\Pi_u \rightarrow X^2\Pi_g$, whose fine structure has been attributed to bending induced by collisions with $He^+$.[21] $V_{in} = 1.07$ kV rms.

of the reaction is plotted as insets of Figure 2a and b. The efficiency of $CO_2$ dissociation decreases with increasing input voltage and inverse flowrate, with the inverse flowrate relationship being nearly linear. These trends are opposite to those obtained for conversion, suggesting that the power (in the case of the input voltage) and yield (in the case of the flow rate dependence) have a greater dependence on these parameters than the conversion.

In an effort to understand the mechanism of $CO_2$ decomposition, optical emission spectroscopy studies of the plasmas were undertaken. Figure 3 illustrates the effect of the addition of $CO_2$ to a pure helium plasma. As small amounts of $CO_2$ are introduced, large changes are observed in the relative intensities of the He emission lines. Additionally, broad peaks due to emission from $CO^+$ (not shown) and $CO_2^+$ (see inset) grow in.[21] This suggests that excited-state He plays a role in the $CO_2$ decomposition reaction and is consistent with established mechanisms of charge and/or energy transfer from He species ($He^+$ and $He_2^+$) to $CO_2$ as a dominant pathway in the ultimate decomposition of $CO_2$.[21−23] Consistent with this observation, the role of the diluent gas is found to have a pronounced effect on the conversion of $CO_2$. $CO_2$ conversions of 19.6% and 13.5% were obtained for Ar and $N_2$, respectively, in the Rh reactor relative to 30.5% obtained under identical conditions in He. This order of reactivity is consistent with the rate constants for bimolecular energy transfer to $CO_2$: $16 \times 10^{-10}$ cm$^3$/s ($He_2^+$),[23] $11 \times 10^{-10}$ cm$^3$/s ($Ar_2^+$),[24] and $7.7 \times 10^{-10}$ cm$^3$/s ($N_2^+$).[24]

Optical emission spectroscopy was also used to understand the unique role the metal plays in $CO_2$ conversion. The relative intensities of He emission lines in a pure He plasma show a strong dependence upon the identity of the metal. In contrast, the relative intensities of the He emission lines in a 2.5% $CO_2$

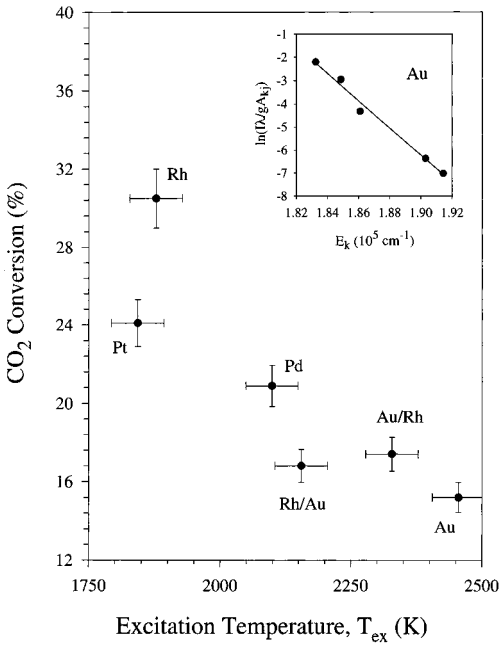


**Figure 4.** Plot of $CO_2$ conversion as a function of the excitation temperature $T_{ex}$ (proportional to the electron temperature $T_e$)[25] for different metal coated reactors. The inset shows the plot of $\ln(I\lambda/gA_{kj})$ vs $E_k$ for gold, from which the Boltzmann slope ($-1/kT_{ex}$) is obtained ($I$ = intensity of the He emission line, $\lambda$ = wavelength of the emission; $g$ = statistical weight of the level, $A_{kj}$ = transition probability, $E_k$ = excitation energy of the upper level).

in He plasma are the same for all metal electrodes examined, suggesting that $CO_2$ has a leveling effect on the distribution of electronic states of He, which is independent of the reactor metal. The Boltzmann plot method[25] was employed in order to compare the excitation temperatures $T_{ex}$ in pure He plasmas as a function of the metal. The excitation temperature is a combination of vibrational, rotational, and electron temperatures of the plasma and can be obtained from the distribution of excited states of He, measured from the intensities of the emission lines of He (see Figure 4, inset). The relationship between integrated line intensity $I$ and excitation temperature $T_{ex}$ is $\ln(I\lambda/gA_{kj}) = -E_k/k_BT_{ex}$, where $\lambda$ is the wavelength of emission, g is the statistical weight of the level, $A_{kj}$ is the transition probability, $E_k$ is the energy of the upper level, and $k_B$ is the Boltzmann constant. Ideally, the electron temperature is determined, but this can be difficult in plasmas that are not in local thermodynamic equilibrium.[25] It is likely that the $T_{ex}$ values underestimate the electron temperature of the plasma, but they are reliable to $\pm$ 5% and should be proportional to the electron temperature. The correlation between $T_{ex}$, and the percent conversion of $CO_2$, is presented in Figure 4. Generally, decreasing electron temperature in a pure helium plasma correlates with increasing conversion of $CO_2$ in low concentration mixtures of $CO_2$ in He.

The role of the metal in the decomposition of $CO_2$, was additionally probed by investigating mixed metal systems, in which the rotor and stator were coated with different metals. Reactors of Rh/Au and Au/Rh (stator/rotor) were chosen, as these metals represent the best (Rh) and poorest (Au) reactivity of the metals studied. Both mixed metal reactors give nearly identical conversions: 17.4% for Au/Rh and 16.8% for Rh/Au, conversions only slightly better than that obtained with the pure gold reactor (15.2%) and nowhere near those obtained with a pure rhodium reactor (30.5%). Furthermore, as can be seen from Figure 4, $T_{ex}$ values for these two reactors fall between values obtained for Au and Pd. Thus, the relative importance of the metal coated on the rotor vs the stator electrode appears to be the same and the reactivity is defined by the poorest activity electrode.

**TABLE 2: Conversion of NO and $H_2O$ as a Function of Electrode Metal Coating**[a]

| metal | NO conversion (%) | $H_2O$ conversion (%) |
|---|---|---|
| Fe | 73 | 29 |
| Pt | 74 | 38 |
| Ni | 80 | 27 |
| Cu | 81 | 36 |
| Pd | 84 | 43 |
| Rh | 89 | 45 |

[a] Conditions for NO: 1.0% NO in He, 80 cc/min (0.0125 min/cc), $V_{in}$ = 1.29 kV rms. Conditions for $H_2O$: 2.9% $H_2O$ in He, except for Pt (3.1% $H_2O$ in He), 20 cc/min, $V_{in}$ = 1.29 kV rms.

Metal effects have been observed in various plasma processes, including ozone synthesis and the synthesis of ammonia and hydrazine.[26−28] Unlike some other studies, we find no correlation between conversion and the work function of the metal,[28] and the differing behavior among the metal electrodes studied here cannot be understood in terms of a specific property of the metal electrode. Under our conditions these metal surfaces, except for Au, are likely oxidized and such correlations may not be observed. It is clear that the electron temperatures of the plasmas of various metal electrodes are different and influence the activation of $CO_2$. These differences are likely due to the contributions of a number of different intrinsic metal parameters, including specific heat, ionization potential, and sticking coefficient. Alternatively, the metal coated surfaces may be acting as catalytic sites. Sputtering in these systems may occur, which would produce gas-phase metal atoms or clusters and might account for differences in reactivity. However, XPS studies of Cu plates placed at the back of the Au/Rh reactor were unable to verify the presence of either Au or Rh sputtered atoms or clusters, suggesting that sputtering is minimal under the conditions employed in our reactions.

**$NO_x$ Remediation**. $NO_x$ from combustion emissions is a precursor to $HNO_3$, a main component of acid rain and fog,[29] and an integral part of the cycle for formation of ground level ozone,[30] which, in addition to being a greenhouse gas, has been linked to reduced crop yields.[31] New, efficient routes to $NO_x$ decomposition are of increasing importance as the environmental demands of higher fuel efficiency promote the use of fuel lean and air rich streams where the production of nitrogen oxides is favored. ac glow discharge studies for the decomposition of NO show some analogies to this research on $CO_2$. High conversions, the ability to operate at atmospheric pressure, and dependence on parameters such as input voltage, flow rate, and type of metal coating on the electrodes are observed, and representative data are presented in Table 2. Some differences are clear with respect to $CO_2$, such as the order of activity of specific metals (Rh > Pd > Cu $\sim$ Ni > Pt $\sim$ Fe), and the extent of activity (up to 100% in this case). Effective, direct total decomposition of NO of 250−10000 ppm has been achieved.

The selectivity of NO decomposition markedly depends on the presence and concentration of $O_2$ in the feed. As illustrated in Figure 5, with no added $O_2$, the main products are $N_2$ and $O_2$, $N_2O$ and $NO_2$ are formed to a lesser extent. Addition of > 0.5% $O_2$ to the 1.0% NO feed results in increasing conversion of NO with an increased selectivity to $N_2O$ and $NO_2$. Formation of nitrogen oxides is expected in the presence of $O_2$ in the feed and $N_2O$ appears to be the initial intermediate in the product distribution curves, evidenced by the maximum in the selectivity

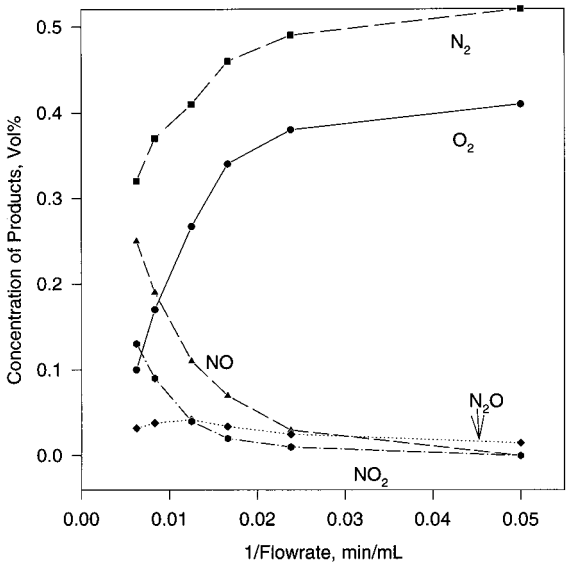


**Figure 5.** Plot of the decomposition of NO (1.0% in He) and formation of nitrogen oxides, $N_2$, and $O_2$ as a function of inverse flow rate with an ac glow discharge produced with Rh electrodes, $V_{in} = 1.29$ kV rms. The oxidation of the rubber coating of the wires of the reactor leads to the partial consumption of oxygen, resulting in formation of up to 0.15% of $CO/CO_2$ as products.

to $N_2O$ (Figure 5). This is somewhat surprising since $N_2O$ in thermal reactions forms at higher temperatures than other nitrogen oxides. The ability to form $N_2O$ is important as a general anesthetic, as a fuel, and as a chemical reactant in catalysis such as in the partial oxidation of methane.[32]

**Water Splitting**. Water splitting is an important reaction which may find use in future fuel cell applications for generation of electricity, and as a possible source of $H_2$ as a fuel.[5] ac glow discharge activation of $H_2O$ (2.9−3.1% in He) leads to decomposition to $H_2$ and $O_2$ and selected conversion results are presented in Table 2. In this case, the order of reactivity of metals is Rh ∼ Pd > Pt ∼ Cu > Fe ∼ Ni. The most important parameters for decomposition of $H_2O$ are flow rate, input voltage, diluent gas, and concentration of water. As is observed for other reactions studied here, conversions increase with increasing input voltage (18% at 0.440 kV rms vs 38% at 1.29 kV rms for Pt) and decreasing flow rate (38% at 20 $cm^3$/min vs 11% at 60 $cm^3$/min for Pt). The conversion order as a function of diluent gas is He > Ar > $N_2$ and, similar to the case for $CO_2$, conversions double when $N_2$ is replaced by He. With a Pt reactor, the hydrogen yield increases from 8% at water concentrations of 20% to a 54% yield for a 1.5% concentration of water. At still lower concentrations of water (<1.5%), conversions of greater than 60% can be obtained.

## Conclusions

We have used glow discharge plasma reactors featuring rotating and stator electrodes coated with Au, Rh, Pt, Pd, Cu, Ni, and Fe for the dissociation of $CO_2$, NO and $H_2O$. For 2.5% $CO_2$ feed, conversions of up to 30.5% could be obtained and the conversions are observed to increase with increasing input voltage and decreasing flow rate. Spectroscopic studies indicate that the electron temperature of the plasmas can be correlated to the observed conversions for $CO_2$. Significant activity has been observed for the exothermic dissociation of NO to $N_2$ and $O_2$. Concentrations of 250−10000 ppm can be dissociated with 100% conversion and substantial amounts of nitrous oxide are formed as an intermediate. The formation of hydrogen and oxygen from water has the same dependence upon flow rate and input voltage observed as that for decomposition of $CO_2$. The best conversions and selectivites for water splitting are obtained at high voltages, low flow rates, and low concentrations of water. Greater than 60% conversion can be obtained for water concentrations of <1.5%.

While the above data are limited, we have used ac glow discharge reactors to study a variety of other reactions, including activation of $CH_4$ and higher hydrocarbons such as $C_2H_6$, preparation of inorganic materials such as amorphous silicon,[33] and in selective oxidations. With the exception of selective oxidations, promising results as regards activity and selectivity to desirable products have been achieved. Just as for the reaction data presented here for $CO_2$, NO, and $H_2O$, the order of activity for different electrode metals is reaction specific. It is not exactly clear why this is so. Optical emission, chemical, and surface analysis data suggest that metal from the electrode surface, if it enters the gas phase, is at undetectable concentrations and either redeposits on the electrode surface or migration of metal occurs along the solid surface.

A further advantage in these types of plasmas is that insulators can be deposited on the surface of the electrodes which do not cause significant problems with charging. For reactions such as selective oxidations and other reactions, use of insulating catalysts and supports such as alumina, silica, and zeolites may significantly alter product distributions. Future work will be aimed at understanding the interactions between activity and intermediates, further elucidation of the role of the metal coating on conversion and selectivity, and studies of new catalyst coatings, and reactor designs.

**Acknowledgment.** The authors acknowledge helpful discussions with Professor G. Roussy of Université Postal Henri Poincaré, Professor J. K. S. Wan of Queen's University, R. Meyer of ASTEX, Inc., and M. C. Quintero and A. Sola of the University of Córdoba. We would also like to thank Mr. Guanguang Xia for assistance with the electrical circuit design, Dr. Venkat V. Krishnan for help with the MS setup, and Mr. Jeff Rozak for assistance with the power measurements. We acknowledge Hokushin Co., Honda Research and Development Corporation, and Fujitsu, Ltd., for support of this research.

## References and Notes

(1) Herman, R. G.; Sun, Q.; Shi, C.; Klier, K.; Wang, C.-B.; Hu, H.; Wachs, I. E.; Bhasin, M. M. *Catal. Today* **1997**, *37*, 1.

(2) Inui, T. *Catal. Today* **1996**, *29*, 329.

(3) Papp, H.; Schuler, P. Zhuang, Q. *Top. Catal.* **1996**, *3*, 299.

(4) Mark, M. F.; Maier, W. F. *J. Catal.* **1996**, *164*, 122.

(5) Rüttinger, W.; Dismukes, G. C. *Chem. Rev.* **1997**, *97*, 1.

(6) Chang, J.-S.; Park, S.-E.; Chon, H. *Appl. Catal. A.* **1996**, *145*, 111.

(7) Büchner, W.; Schliebs, R.; Winter, G.; Büchel, K. H. *Industrial Inorganic Chemistry*; VCH: Weinheim, 1989.

(8) Weissermel, K.; Arpe, H.-J. *Industrial Organic Chemistry*; Verlag Chemie: New York, 1978.

(9) Fridman, A. A.; Rusanov. V. D. *Pure Appl. Chem.* **1994**, *66*, 1267.

(10) Wan, J. K. S. *Res. Chem. Intermed.* **1993**, *19*, 147. Bamwenda, G.; Moore, E.; Wan, J. K. S. *Res. Chem. Intermed.* **1992**, *17*, 243.

(11) Thiebaut, J. M.; Roussy, G.; Medjram, M.; Seyfield, L. Garin, F.; Maire, *J. Catal. Lett.* **1993**, *21*, 133. Gourari, S.; Roussy, G.; Thiebaut, J. M.; Zoulalian, A. *Chem. Eng. J.* **1992**, *49*, 79.

(12) Reid, D. W. *Res. Chem. Intermed.* **1994**, 97.

(13) Goldman, M.; Goldman, A.; Sigmond, R. S. *Pure Appl. Chem.* **1985**, *57*, 1353.

(14) Chang, J.-S.; Lawless, P. A.; Yamamoto, T. *IEEE Trans. Plasma Sci.* **1991**, *19*, 1152.

(15) Hayashi, Y., Fujitsu, Ltd. U.S. Patent 08/139,907, July 1995. Hayashi, Y., Ohta, H., Yanobe, T., Hokushin Co., Fujitsu, Ltd. U.S. Patent August 1995.

(16) Azar, C.; Rodhe, H. *Science* **1997**, *276*, 1818.
(17) Meehl, G. A.; Washington, W. M. *Nature* **1996**, *382*, 56. Sellers, P. J.; Bounoua, L.; Collatz, G. J.; Randall, D. A.; Dazlich, D. A.; Los, S. O.; Berry, J. A.; Fung, I.; Tucker, C. J.; Field, C. B.; Jensen, T. G. *Science* **1996**, *271*, 1402.
(18) Sarmiento, J. L.; Le Quéré, C. *Science* **1996**, *274*, 1346.
(19) DeSimone, J. M.; Maury, E. E.; Menceloglu, Y. Z.; McClain, J. B.; Romack, T. J.; Combes, J. R. *Science* **1994**, *265*, 356. McClain, J. B.; Betts, D. E.; Canelas, D. A.; Samulski, E. T.; DeSimone, J. M.; Londono, J. D.; Cochran, H. D.; Wignall, G. D.; Chillura-Martino, D.; Triolo, R. *Science* **1996**, *274*, 2049.
(20) Edwards, J. H. *Catal. Today* **1995**, *23*, 59.
(21) Sim, W.; Haugh, M. *J. Chem. Phys*. **1976**, *65*, 1616.
(22) Buser, R. G.; Sullivan, J. J. *J. Appl. Phys*. **1970**, *41*, 472.
(23) Lee, F. W.; Collins, C. B.; Waller, R. A. *J. Chem. Phys.* **1976**, *65*, 1605
(24) Maezono, I.; Chang, J.-S. *IEEE Trans. 1nd. App.* **1990**, *26*, 651
(25) Quintero, M. C.; Rodero, A.; García, M. C.; Sola, A. *Appl. Spectrosc*. **1997**, *51*, 778.
(26) Voblikova, V. A.; Filippov. Y. V.; Vendillo, V. P. *Russ. J. Phys. Chem.* **1980**, *54*, 1416.
(27) Tanaka, S.; Uyama, H.; Matsumoto, O. *Plasma Chem. Plasma Proc.* **1994**, *14*, 491.
(28) Eremin, E. N.; Mal'tsev, A. N.; Belova, V. M. *Russ. J. Phys. Chem.* **1971**, *45*, 205.
(29) Seinfeld, J. H. *Science* **1989**, *243*, 745.
(30) Hough, A. M.; Derwent, R. G. *Nature* **1990**, *344*, 645. Johnson, C. Henshaw, J. McInnes, G. *Nature* **1992**, *355*, 69.
(31) Chameides, W. L.; Kasibhatla, P. S.; Yienger, J.; Levy, H., II *Science* **1994**, *264*, 74.
(32) Hutchings, G. J.; Scurrell, M. S.; Woodhouse, J. R. *Chem. Soc. Rev.* **1989**, *18*, 251.
(33) Giraldo, O. H.; Willis, W. S.; Marquez, M.; Suib, S. L.; Hayashi, Y.; Matsumoto, H. *Chem. Mater*. **1998**, *10*, 366.